pISSN 1229-3008 eISSN 2287-6251
Progress in Superconductivity and Cryogenics
Vol.21, No.3, (2019), pp.22~26 https://doi.org/10.9714/psac.2019.21.3.022

Simulation of superconducting cavities for quantum computing

Seong Hyeon Park, Junyoung An, Jeseok Bang, and Seungyong Hahn*

Department of Electrical and Computer Engineering, Seoul National University, Seoul, 08826, Korea

(Received 14 August 2019; revised or reviewed 18 September 2019; accepted 19 September 2019)

Abstract

With an increasing potential to realize quantum computer, it has recently been an important issue to extend the capabilities of RF cavities to maintain longer coherent quantum system. Using superconductors instead of normal metals allows the quantum system to have a substantially enhanced quality factor. In this paper, surface impedances of superconducting cavities are calculated by the Mattis-Bardeen theory with Python & MATLAB programs. With a simulation of electromagnetic field distribution, the sensitivity to dielectric and surface losses of the superconducting cavities are determined. Then calculations of the resonance frequency and quality factor of three-dimensional superconducting resonators made of Al or Nb are discussed.

Keywords: Mattis-Bardeen theory, Q-factor, quantum computing, RF resonator, surface impedance

1. INTRODUCTION

In recent years, an increase in the number of qubits have shown the possibility of scalable quantum computer. According to circuit quantum electrodynamics (cQED), RF cavities or RF resonators are essential to build a quantum system. A superconducting cavity has high quality factor relative to normal metals, due to the physical properties of superconductors. Thus the cavity can protect qubits from decoherence for a long time [1] and can be used as a quantum memory [2].

Planar resonators – another type of RF resonators show that the degradation of quality factor (Q-factor) compared to 3D bulk cavities in a quantum computing system of sub-millikelvin (-20 mK) with low excitation power [3]. Three-dimensional bulk cavities however, have achieved 22 GHz resonant frequency at 0.15 K [4] and the coupling of qubits to 3D bulk cavities could lead to success of cQED experiments with coherence in milliseconds [2].

To design RF cavities for quantum computing system, it is required to analyze the physical properties of super-conducting resonators in low temperature and which types of losses exist. In this paper, features of aluminum and niobium cavities are major topics to discuss. Analytic calculation methods of properties of superconducting cavities in sub-millikelvin temperature will be discussed. After that, the simulation results will be shown to describe the physical behaviors of superconducting cavities.

2. PROPERTIES OF SUPERCONDUCTING CAVITIES

2.1. Resonant Frequency

Resonant frequency of a RF cavity depends on geometric features of the cavity. Though the surface impedance of superconductors (or normal metals) also effects on the resonant frequency, the frequency shift due to the surface impedance is not dominant [8]. Thus, geometric parameter is a key factor to decide the resonant frequency. In this paper, simple but most common geometries – rectangular and cylindrical are considered.

First, transverse electric (TE) modes of a rectangular cavity will be discussed [5].

Let $F_z(x,y,z)$ is a scalar z component of the vector potential function $\boldsymbol{F}$, $\boldsymbol{F}$ satisfies the Helmholtz equation:

$$\nabla^2 F_z(x,y,z) + \beta^2 F_z(x,y,z) = 0 \tag{1}$$

TE modes to z axis for a rectangular cavity must satisfy the following equations:

$$E_x = -\frac{1}{\epsilon}\frac{\partial F_z}{\partial y}, \quad H_x = -i\frac{1}{\omega\mu\epsilon}\frac{\partial^2 F_z}{\partial x \partial z} \tag{2}$$

$$E_y = \frac{1}{\epsilon}\frac{\partial F_z}{\partial x}, \quad H_y = -i\frac{1}{\omega\mu\epsilon}\frac{\partial^2 F_z}{\partial x \partial z} \tag{3}$$

$$E_z = 0, \quad H_z = -i\frac{1}{\omega\mu\epsilon}\left(\frac{\partial^2}{\partial z^2} + \beta^2\right)F_z \tag{4}$$

For width a, depth b and height c rectangular cavity, β is a constant related to boundary conditions:

$$\beta_x^2 + \beta_y^2 + \beta_z^2 = \beta^2 = \omega^2\mu\epsilon \tag{5}$$

$$\left(\frac{m\pi}{a}\right)^2 + \left(\frac{n\pi}{b}\right)^2 + \left(\frac{p\pi}{c}\right)^2 = (2\pi f_r)^2\mu\epsilon \tag{6}$$

$$(f_r)_{mnp} = \frac{1}{2\pi\sqrt{\mu\epsilon}}\sqrt{\left(\frac{m\pi}{a}\right)^2 + \left(\frac{n\pi}{b}\right)^2 + \left(\frac{p\pi}{c}\right)^2} \tag{7}$$

For a rectangular cavity with $c > a > b$, the dominant mode is the TE_{101}, at which the cavity has the lowest

* Corresponding author: hahnsy@snu.ac.kr

resonant frequency. Thus the resonant frequency of the TE_{101} is represented by

$$(f_r)_{101} = \frac{1}{2\pi\sqrt{\mu\epsilon}}\sqrt{\left(\frac{\pi}{a}\right)^2 + \left(\frac{\pi}{c}\right)^2} \quad (8)$$

TE and TM modes of a cylindrical cavity are similar to that of a rectangular cavity. For radius r and height h cylindrical cavity, the z component of the vector potential $F_z(\rho, \phi, z)$ is

$$F_z^{TE}(\rho, \phi, z) = A_{mn}J_m(\beta'_\rho \rho)\begin{bmatrix}\sin n\phi \\ \cos n\phi\end{bmatrix}\sin(\beta_z z) \quad (9)$$

$$F_z^{TM}(\rho, \phi, z) = A_{mn}J_m(\beta_\rho \rho)\begin{bmatrix}\sin n\phi \\ \cos n\phi\end{bmatrix}\sin(\beta_z z) \quad (10)$$

,where β is a constant related to boundary conditions:

$$\beta'_\rho = \frac{\chi'_{mn}}{r}, \beta_\rho = \frac{\chi_{mn}}{r}, \beta_z = \frac{p\pi}{h} \quad (11)$$

,where J_m is the Bessel function of the first kind,

$$J_m(\chi_{mn}) = 0, J'_m(\chi'_{mn}) = 0 \quad (12)$$

Thus the resonant frequency of cylindrical cavity is

$$f_{mnp}^{TE} = \frac{1}{2\pi\sqrt{\mu\epsilon}}\sqrt{\left(\frac{\chi'_{mn}}{r}\right)^2 + \left(\frac{p\pi}{h}\right)^2} \quad (13)$$

$$f_{mnp}^{TM} = \frac{1}{2\pi\sqrt{\mu\epsilon}}\sqrt{\left(\frac{\chi_{mn}}{r}\right)^2 + \left(\frac{p\pi}{h}\right)^2} \quad (14)$$

When $h/r < 2.03$ the dominant resonant mode is the TM_{010}whereas for $h/r > 2.03$ the dominant mode is the TE_{111} mode. There is no current flowing on the corners of the cavity when the TE_{011} mode is the resonant mode of the cavity [15]. Thus, in this paper, cylindrical cavities of the TE_{011} mode are studied.

2.2. Surface Impedance

When high frequency electromagnetic fields which vary in amplitude over a mean free path is applied to the superconductor, the usual expression of bulk conductivity is no more valid [6]. Thus, the Mattis-Bardeen theory of the anomalous skin effect in superconducting metals is required to calculate the surface impedance.

In the extreme anomalous limit, when the penetration of varying AC fields is smaller than the coherence distance $\xi_0 \sim v_0/\pi\epsilon_0$, the Mattis-Bardeen theory introduced the expressions of surface impedance of a superconductor. Note that v_0 is Fermi velocity and ϵ_0 is an energy gap. Then the ratio of the complex conductivity of the superconducting state to normal state is

$$\frac{\sigma}{\sigma_N} = \frac{\sigma_1 - i\sigma_2}{\sigma_N} = \frac{I(\omega, 0, T)}{-i\pi\hbar\omega} \quad (15)$$

,where $I(\omega, R, T)$ is the current flowing inside the superconductor. Expressions for σ_1 and σ_2 are

$$\frac{\sigma_1}{\sigma_N} = \frac{2}{\hbar\omega}\int_{\epsilon_0}^{\infty}[f(E) - f(E + \hbar\omega)]g(E)dE \quad (16)$$

$$\frac{\sigma_2}{\sigma_N} = \frac{1}{\hbar\omega}\int_{\epsilon_{0-\hbar\omega}}^{\epsilon_0}[f(E) - f(E + \hbar\omega)]g(E)dE \quad (17)$$

,where ϵ_1 and ϵ_2 are the Block energies which are represented by

$$\epsilon_1 = (E^2 - \epsilon_0^2)^{\frac{1}{2}}, \quad \epsilon_2 = [(E + \hbar\omega)^2 - \epsilon_0^2]^{\frac{1}{2}} \quad (18)$$

$f(E)$ is Fermi-Dirac distribution and $g(E)$ is

$$g(E) = \frac{E^2 + \epsilon_0^2 + \hbar\omega E}{\epsilon_1\epsilon_2} \quad (19)$$

Numerous superconductors including ceramics [9, 11] and thin films of HTS were fitted well to the Mattis-Bardeen theory [19]. However, since the ξ of HTS is usually smaller than the electron mean free math l, we need another method to calculate the surface impedance. In this paper, we used microscopic expressions derived by Zimmermann to calculate superconductors' complex conductivity and surface impedance [17]

$$\sigma(\omega) = \frac{i\sigma_N}{2\omega\tau}\left[\int_{\Delta}^{\Delta+\hbar\omega} I_1 dE + \int_{\Delta}^{\infty} I_2 dE\right] \quad (20)$$

$$I_1 = \tanh\frac{E}{2kT}\left\{\left[1 - \frac{\Delta^2 + E(E - \hbar\omega)}{P_4P_2}\right]\frac{1}{P_4 - P_2 + \frac{i}{\tau}} - \left[1 + \frac{\Delta^2 + E(E + \hbar\omega)}{P_4P_2}\right]\frac{1}{P_3 - P_2 + \frac{i}{\tau}}\right\} \quad (21)$$

$$I_2 = \tanh\frac{E + \hbar\omega}{2kT}\left\{\left[1 - \frac{\Delta^2 + E(E + \hbar\omega)}{P_1P_2}\right]\frac{1}{P_1 - P_2 + \frac{i}{\tau}} - \left[1 - \frac{\Delta^2 + E(E + \hbar\omega)}{P_1P_2}\right]\frac{1}{-P_1 - P_2 + \frac{i}{\tau}}\right\} + \tanh\frac{E}{2kT}\left\{\left[1 - \frac{\Delta^2 + E(E + \hbar\omega)}{P_1P_2}\right]\frac{1}{P_1 + P_2 + \frac{i}{\tau}} - \left[1 + \frac{\Delta^2 + E(E + \hbar\omega)}{P_1P_2}\right]\frac{1}{P_1 - P_2 + \frac{i}{\tau}}\right\} \quad (22)$$

where $P_1 = \sqrt{(E + \hbar\omega)^2 - \Delta^2}, P_2 = \sqrt{E^2 - \Delta^2}$, $P_3 = \sqrt{(E - \hbar\omega)^2 - \Delta^2}$, $P_4 = i\sqrt{\Delta^2 - (E - \hbar\omega)^2}$ and Δ is gap energy.

Finally, the surface impedance of the superconductor can be obtained by the following equation

$$Z_s = \sqrt{\frac{i\mu_0\omega}{\sigma_1 - i\sigma_2}} = R_s + iX_s \quad (23)$$

To estimate the performance of superconducting cavities more precisely, we assumed that R_s is a sum of resistance derived from BCS theory and the residual resistance. Thus, the surface impedance is

$$Z_s = R_s + iX_s = (R_{BCS} + R_{res}) + iX_s \quad (24)$$

2.3. Quality Factor

Q-factor is a key value to figure out how long the cavity can hold the coherent state of quantum system. For example, lifetime of a photon is proportional to Q-factor, $\tau_{int} = Q_{int}/\omega$ [8]. If we assume that there are no other losses except the conduction loss of the metal, then the calculation of the Q-factor would be much easier. However, if we measure the Q-factor of the cavity in the laboratory, there would be huge difference between the analytical calculation and the measured value. Though without bulk dielectric or impurities, there are still two types of loss that can be neglected. These losses are associated with surface imperfections and the inherent physical properties of a superconductor [8].

First, the metal walls with a thin oxide layer which has a dielectric loss tangent. Let the cavity is only damped by an oxide layer of thickness t and $Q_{diel} = 1/\tan\delta$. Then the Q-factor by an oxide dielectric layer is [5]

$$Q_E = \frac{Q_{diel}\int_V |E|^2 dV}{\epsilon_r t \int_S |E|^2 dS} = \frac{Q_{diel}}{p_{diel}} \quad (25)$$

, where p_{diel} is the surface dielectric participation ratio of the cavity. We assume that the thickness of an oxide layer is about 1 nm and tan δ is 10^{-3} inferred from [9].

Second, a cavity has conduction losses due to the surface impedance of the superconductor. A superconducting cavity has a finite surface impedance that can't be neglected when calculating Q-factor. The cavity's Q-factor by the surface impedance is [5]

$$Q_H = \frac{\omega\mu\lambda \int_V |H|^2 dV}{R_s \int_S |H|^2 dS} = \frac{Q_s}{\alpha} \quad (26)$$

,where $\omega\mu\lambda/R_s$ is surface Q-factor and α is magnetic participation ratio. Thus, expression of the internal quality factor of the cavity is

$$\frac{1}{Q_{int}} = \frac{1}{Q_E} + \frac{1}{Q_H} \quad (27)$$

2.4. Resonant Frequency Shift

As mentioned above, resonant frequency of 3D RF cavity depends on its geometric features. However, as the temperature rises from the absolute zero temperature, the surface impedance changes exponentially. Though the percentage of changes in resonant frequency is small, predicting the exact shifted resonant frequency is important since, Q-factor of superconducting cavity is usually over 10^8.

The Mattis-Bardeen theory of complex conductivity predicted the relations of resonant frequency shifts due to the change of the surface impedance and Q-factor [8, 20]. The estimation of the resonant frequency shift as a function of temperature by [18] is as follows.

$$\delta\frac{1}{Q} + 2i\frac{\delta f}{f} = \frac{\alpha}{\omega\mu\lambda_0}(\delta R_s + i\delta X_s) \quad (28)$$

, where α is geometric factor.

3. RESULTS AND DISCUSSIONS

To calculate complex conductivity and surface impedance of superconducting cavities, physical properties of the materials such as T_C , Δ_0 , λ_0 and geometric parameters are necessary. In this paper, we analyzed 4 types of superconductors – aluminum, niobium, Nb3Sn and TiN. The parameters are shown in Table I.

TABLE I
PHYSICAL PROPERTIES OF VARIOUS SUPERCONDUCTORS [10-16].

Material Properties	Unit	Aluminum	Niobium	Nb3Sn	TiN
T_c	[K]	1.2	9.2	18	5.6
v_f	[m/s]	13.4×10^5	0.28×10^5	0.99×10^5	7×10^5
λ_0	[nm]	15.4	33.3	60	50
l	[nm]	10000	20	1	45
Δ_0/k_BT_c	[.]	1.76	1.76	2.25	1.81

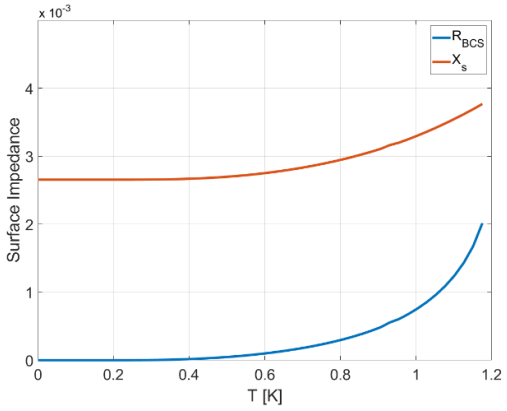

Fig. 1. Real and imaginary part of surface impedance of aluminum at 11.48 GHz as a function of temperature. Real part of surface impedance converges to zero when the temperature goes to absolute zero.

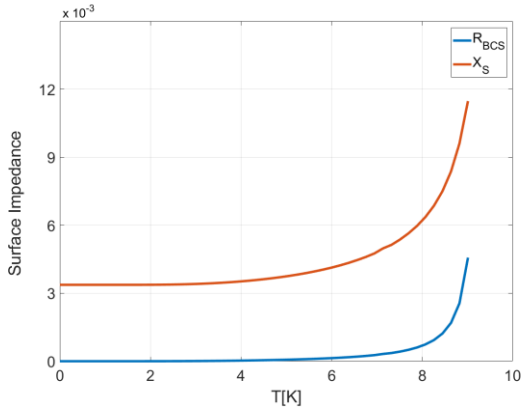

Fig. 2. Real and imaginary part of surface impedance of niobium at 11.48 GHz as a function of temperature. Real part of surface impedance converges to zero when the temperature goes to absolute zero.

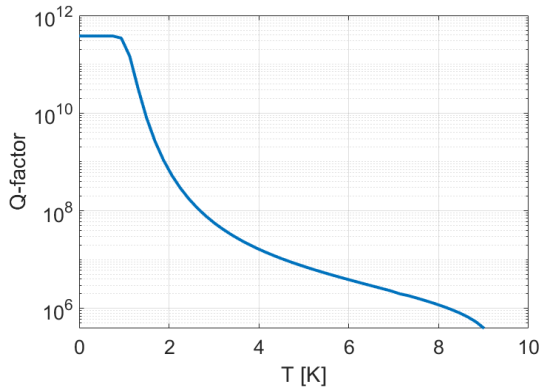

Fig. 3. Estimation of the Q-factor of niobium cylindrical cavity TE_{011} mode as a function of the temperature.

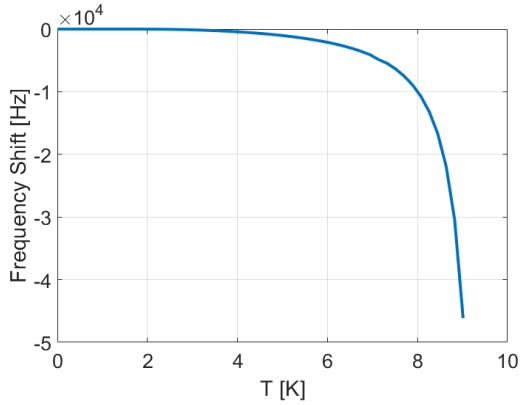

Fig. 4. Resonant frequency shifts of Nb cylindrical cavity derived by the Mattis-Bardeen theory.

Temperature dependences of the surface impedances of aluminum and niobium are shown in Fig. 1 and Fig. 2 respectively.

As shown in Fig.1 and Fig. 2, R_S converges to R_{res} when temperature goes to 0 K. However, as the temperature goes to the critical temperature, R_{BCS} exponentially increases. A plot of the Q-factor of aluminum cavity with radius 20 mm and height 20 mm as a function of temperature is shown in Fig. 3.

The relation between the temperature and R_{BCS} shows that cavities should be located in low temperature to maintain the quantum computing system stable as long as possible. In Fig. 3, the saturation of Q-factor is discovered as the temperature goes to 0 K. This is because R_S starts to saturate near 0 K and R_S converges to residual resistance. Due to the finite surface impedance of the superconducting cavity, the resonant frequency shifts to lower. Though the change of the resonant frequency is relatively small compared to the magnitude of the resonant frequency, with the Q-factor being over 10^8, estimation of the exact change in the resonant frequency is important for operating quantum computing systems efficiently. In Fig. 4, the change in the resonant frequency of superconducting cavity is estimated by the Mattis-Bardeen theory.

Lastly, we focus on the geometries of the cavities which are compatible with general cQED prototypes for quantum computing experiments at about 10 GHz and 20 mK. The geometric parameters, resonant frequencies and Q-factors at 20 mK are shown in Table II.

TABLE II
Q-FACTORS OF VARIOUS CAVITIES.

Cavity Type (Material)	Resonant Mode	Resonant Frequency [GHz]	Q-factor
Cylindrical (Al)	TM_{010}	11.47	2.71×10^{10}
Cylindrical (Nb)	TM_{010}	11.47	1.73×10^{11}
Cylindrical (Al)	TE_{011}	10.85	2.81×10^{10}
Cylindrical (Nb)	TE_{011}	10.85	3.78×10^{11}
Rectangular (Al)	TE_{101}	11.17	3.94×10^{8}
Rectangular (Nb)	TE_{101}	11.17	2.60×10^{9}

With several simulations, cylindrical cavities show higher Q-factor than rectangular cavities for 11 GHz of resonant frequency. For cylindrical cavity, TE_{011} mode shows higher Q-factor than TM_{010} due to low participation ratio at similar resonant frequency due to its electromagnetic field distribution. Generally, niobium cavities result in better Q-factor than aluminum cavities. Thus, with Nb cylindrical cavity for TE_{011} mode, it is possible to achieve an extremely high Q-factor that can't be imagined in normal metal cavities.

4. CONCLUISION

We have studied and simulated superconducting 3D cavities for quantum computing system. With a small participation ratio of the surfaces of TE_{011} cylindrical cavities, it is shown that reaching Q-factor above 10^{11} and over a second of photon lifetime may be possible for a high-purity Nb cavity.

ACKNOWLEDGMENT

This research was supported by Samsung Electronics.

REFERENCES

[1] A. A. Houck, et al., "Controlling the spontaneous emission of a superconducting transmon qubit," *Physical review letters*, vol. 101, pp. 080502, 2008.
[2] M. Reagor, et al., "Quantum memory with millisecond coherence in circuit QED," *Physical Review B*, vol. 94, pp. 014506, 2016.
[3] J. M. Sage, et al., "Study of loss in superconducting coplanar waveguide resonators," *Journal of Applied Physics*, vol. 109, pp. 063915, 2011.
[4] S. Brattke, B. T. Varcoe, and H. Walther, "Generation of photon number states on demand via cavity quantum electrodynamics," *Physical review letters*, vol. 86, pp. 3534, 2001.
[5] C. A. Balanis, *Advanced engineering electromagnetics*, John Wiley & Sons, 1999.
[6] D. C. Mattis and J. Bardeen, "Theory of the anomalous skin effect in normal and superconducting metals," *Physical Review*, vol. 111, pp. 412, 1958.
[7] M. Reagor, et al. "Reaching 10 ms single photon lifetimes for superconducting aluminum cavities," *Applied Physics Letters*, 102, 2013: 192604.
[8] M. Reagor, et al. "Reaching 10 ms single photon lifetimes for superconducting aluminum cavities," *Applied Physics Letters*, 102, 2013: 192604.

[9] J. Zmuidzinas, "Superconducting microresonators: Physics and applications," *Annu. Rev. Condens. Matter Phys*, vol. 3, pp. 169-214, 2012.
[10] J. Halbritter, "Comparison between measured and calculatedRF losses in the superconducting state," *Zeitschrift für Physik*, vol. 238, pp. 466-476, 1970.
[11] J. P. Turneaure, J. Halbritter and H. A. Schwettman, "The surface impedance of superconductors and normal conductors: The Mattis-Bardeen theory," *Journal of Superconductivity*, vol. 4, pp. 341-355, 1991.
[12] J. Weibler, et al., "Properties of Metals used for RF shielding," *EMC Test and Design*, pp. 100, 1993.
[13] C. Kittel, et al., *Introduction to solid state physics*, New York: Wiley, 1976.
[14] A. Kardakova, et al., "The electron phonon relaxation time in thin superconducting titanium nitride films," *Applied Physics Letters*, vol. 103, pp. 252602, 2013.
[15] J. P. Turneaure and I. Weissman, "Microwave surface resistance of superconducting niobium," *Journal of Applied Physics*, vol. 39, pp. 4417-4427, 1968.
[16] H. Padamsee, et al., *RF superconductivity for accelerators*, New York: Wiley vch, 2011.
[17] W. Zimmermann, et al., "Optical conductivity of BCS superconductors with arbitrary purity," *Physica C: Superconductivity*, vol. 183, pp. 99-104, 1991.
[18] J. C. Slater and J. Clarke, "Microwave electronics," *Reviews of Modern Physics*, vol. 18, pp. 441-512, 1946.
[19] M. Tinkham, "Far infrared absorption in superconductors," *Far-Infrared Properties of Solids*, Springer, Boston, MA, pp. 223-246, 1970.
[20] D. E. Oates, et al., "Surface-impedance measurements of superconducting NbN films," *Physical Review B*, vol. 43, pp. 7655-7663, 1991.